BMB
*Reports*

**BMB Rep. 2014; 47(1): 15-20**
www.bmbreports.org

# Mutation of the *lbp-5* gene alters metabolic output in *Caenorhabditis elegans*

*Mo Xu, Eun-Young Choi & Young-Ki Paik**

Department of Biochemistry and Department of the Integrated Omics for the Biomedical Science, WCU Program, College of Life Science and Biotechnology, Yonsei Proteome Research Center, Yonsei University, Seoul 120-749, Korea

**Intracellular lipid-binding proteins (LBPs) impact fatty acid homeostasis in various ways, including fatty acid transport into mitochondria. However, the physiological consequences caused by mutations in genes encoding LBPs remain largely uncharacterized. Here, we explore the metabolic consequences of *lbp-5* gene deficiency in terms of energy homeostasis in *Caenorhabditis elegans*. In addition to increased fat storage, which has previously been reported, deletion of *lbp-5* attenuated mitochondrial membrane potential and increased reactive oxygen species levels. Biochemical measurement coupled to proteomic analysis of the *lbp-5*(*tm1618*) mutant revealed highly increased rates of glycolysis in this mutant. These differential expression profile data support a novel metabolic adaptation of *C. elegans*, in which glycolysis is activated to compensate for the energy shortage due to the insufficient mitochondrial β-oxidation of fatty acids in *lbp-5* mutant worms. This report marks the first demonstration of a unique metabolic adaptation that is a consequence of LBP-5 deficiency in *C. elegans*. [BMB Reports 2014; 47(1): 15-20]**

## INTRODUCTION

Fatty acids play many important roles in various cellular processes and in nutritional balance (1, 2). Because fatty acids are hydrophobic molecules, they are solubilized and transported within the cell mainly by specific lipid-binding proteins (LBPs) in *C. elegans* and by lipid chaperones termed fatty acid-binding proteins (FABPs) in mammals (3, 4). These proteins are also involved in targeting fatty acids to specific metabolic regulatory pathways and in controlling gene expression during cell growth (5), influencing energy homeostasis (5, 6).

We previously investigated the novel functions of LBPs in energy homeostasis *in vivo* through RNA interference (RNAi) of *C. elegans lbp* genes (*lbp-1* to *-9*) and found that fat accumulation was most pronounced in worms with silenced or mutated *lbp-5* (7), which was one of the nine genes studied. This was further supported by the severe fat accumulation observed in worms with the *lbp-5*(*tm1618*) mutant (7), suggesting insufficient transport of fatty acids to the mitochondria for β-oxidation.

However, little is known about the roles of LBPs in other related cellular metabolic processes, such as glycolysis and the tricarboxylic acid (TCA) cycle. We address this issue by introducing a nonfunctional *lbp-5* mutant and analyzing the consequences of losing the function provided by *lbp-5* mutant in related metabolic pathways, such as glycolysis. Furthermore, we hypothesize that improper regulation or disruption of cellular lipid transport by LBPs would alter the metabolic processes in a compensatory mechanism to maintain energy homeostasis in *C. elegans*.

Here, we present evidence that when the intracellular lipid chaperone gene *lbp-5* is disrupted, *C. elegans* suffers from functional attenuation of the mitochondria-where fatty acids are usually metabolized to provide energy-but metabolically adapts by activating aerobic glycolysis to overcome the energy shortage.

## RESULTS

### Mutation of *lbp-5* in *C. elegans* causes significant metabolic alterations

Previously, it was found that RNAi-mediated knockdown or mutation of *lbp-5* caused more fat accumulation in *C. elegans* than the disruption of other members of the LBP family did (7). To better understand the role of *lbp-5* in energy metabolism, we performed a series of biochemical assays to assess the state of energy homeostasis in *lbp-5*(*tm1618*) mutant worms (Supplemental Information). First, to evaluate the efficiency of energy production in mitochondria, ΔΨm was determined using the TMRE uptake in the *lbp-5*(*tm1618*) mutant and N2 worms (8). Surprisingly, the ΔΨm in *lbp-5*(*tm1618*) mutant worms was much lower than that in N2 worms according to TMRE uptake (Fig. 1A, B). This result suggests the influence of reduction in energy production on other metabolic pathways.

To investigate this, we assessed the rate of glycolysis using the conventional lactate dehydrogenase (LDH) activity assay.

*Corresponding author. Tel: +82-2-2123-4242; Fax: +82-2-393-6589; E-mail: paikyk@yonsei.ac.kr

http://dx.doi.org/10.5483/BMBRep.2014.47.1.086

**Received 17 April 2013, Revised 30 April 2013, Accepted 2 May 2013**

**Keywords:** *C. elegans*, Fatty acid metabolism, *lbp-5*, Obesity

ISSN: 1976-670X (electronic edition)

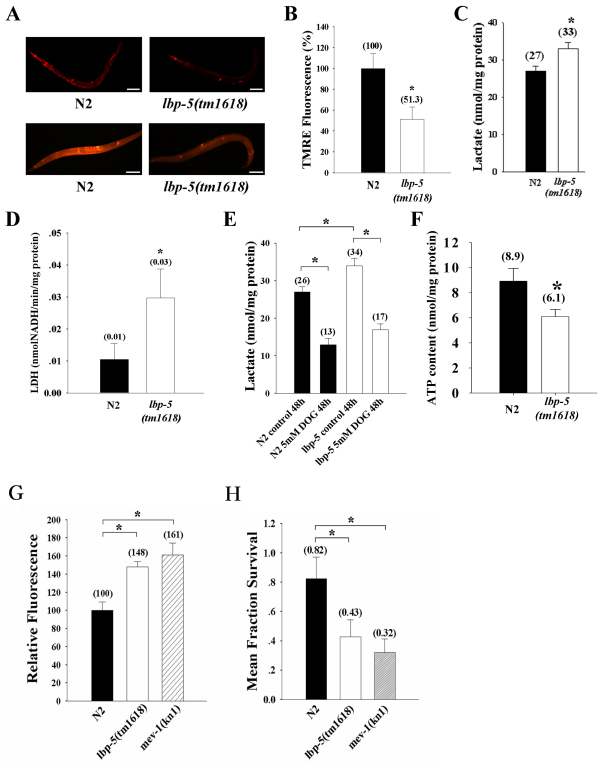


**Fig. 1.** Metabolic consequences of *lbp-5* deficiency in *Caenorhabditis elegans*. (A) Deletion of *lbp-5* decreases mitochondrial membrane potential. Confocal (upper panel) and fluorescence (lower panel) images of tetramethylrhodamine ethyl ester (TMRE)-stained nematodes. Scale bars, 100 $\mu$m. (B) Quantification of the data shown in (A). (C) Levels of lactate production in *lbp-5*(*tm1618*) mutant and control N2 worms. (D) Levels of lactate dehydrogenase activity in *lbp-5*(*tm1618*) mutant and control N2 worms. (E) The effect of deoxyglucose treatment on lactate production in *lbp-5*(*tm1618*) mutant and control N2 worms. (F) Deletion of *lbp-5* decreases ATP levels in adult nematodes compared with N2 worms. (G) Effect of *lbp-5* mutation on ROS levels. Intracellular ROS levels in mutant and control worms were measured by MitoSOX. (H) Effect of paraquat treatment on the survival of mutant and control worms. The number of living worms was counted 72 h after treatment with 4 mM paraquat. The *mev-1*(*kn1*) mutant was used as the positive control. Data represent the mean ± SD of at least three measurements from three independent experiments. *P < 0.05 as calculated by Student's t-test versus the control sample.

Additionally, we also measured lactate production levels by comparing the accumulation of L-(+)-lactate, a major stereo-isomer of lactate formed during glycolysis, between mutant and control worms. Our results showed that the bodies of *lbp-5*(*tm1618*) mutant worms contained approximately 22% (33 ±1.7 vs. 27 ±1.4 nmol/mg protein; n = 3) more lactate than those of N2 worms (Fig. 1C). Consistent with this finding, our examination revealed 3-fold higher LDH activity in *lbp-5*(*tm1618*) mutants than in N2 worms (Fig. 1D). Measurement of lactate production following treatment with DOG (17), an inhibitor of glycolysis, demonstrated the connection between the increased lactate production and glycolysis (Fig. 1E). Finally, *lbp-5* mutant worms exhibited lower ATP levels than N2 worms, implying that energy production were repressed in *lbp-5* mutant worms (Fig. 1F). These results demonstrate that *lbp-5* deletion causes a reduction in mitochondrial function but induces a substantial increase in the rate of glycolysis in aerobically cultured worms.

## Deficiency of *lbp-5* leads to increased reactive oxygen species (ROS) production

Based on the observed suppression of mitochondrial function (Fig. 1A and B), we hypothesized that reduced mitochondrial potential may also accompany compromised anti-oxidant activity. To test this hypothesis, we compared the ROS levels (18) between *lbp-5*(*tm1618*) mutant and N2 worms by using *mev-1*(*kn1*) mutant worms as the positive control (Supplemental Information). The *mev-1* gene encodes the cytochrome *b* large subunit in complex II of the mitochondrial electron transport chain. Thus, *mev-1*(*kn1*) worms display increased levels of superoxide in the mitochondria and sensitivity to paraquat, a superoxide generator frequently used to examine ROS resistance. We found that *lbp-5* deficiency led to approximately 48% higher ROS levels in the *lbp-5*(*tm1618*) worms than those of the control worms (Fig. 1G). These higher ROS levels are quite similar to the levels found in *mev-1*(*kn1*) worms (61% higher than the levels in N2 worms). For further confirmation, we measured sensitivity to paraquat by testing the ability of adults to survive in the presence of a high concentration of the compound (4 mM). The *lbp-5*(*tm1618*) mutant worms showed decreased survival with paraquat treatment (Fig. 1H). This result suggests a link between the inability to transport fatty acids in the *lbp-5* mutant and the attenuated mitochondrial anti-oxidant function (9). These data also indicate that the reduction in fatty acid transport in this mutant may weaken mitochondrial protection against ROS produced by paraquat.

## Proteomic analysis of *lbp-5* deficiency in *C. elegans* supports the basis for metabolic adaptation

To explore the mechanism by which *lbp-5* deficiency not only alters cellular metabolism by augmenting the rate of glycolysis but also suppresses mitochondrial function, we conducted a proteomic analysis of *lbp-5*(*tm1618*) mutant and N2 wild-type worms (Supplemental Information). This proteomic analysis was designed to evaluate changes in protein abundance and measure the expression of representative genes involved in energy metabolism and oxidative stress. First, differences in protein levels between the two worm strains (N2 vs. the *lbp-5* mutant) were documented through 2DE and mass spectrometry (MS) analysis (Fig. S1) (19). Because most enzymes involved in energy metabolism are soluble proteins, it was thought that 2DE would facilitate the detection of changes in the expression of proteins involved in energy metabolism in the

**Table 1.** Proteins identified to be differentially expressed between N2 and *lbp-5*(*tm1618*) nematodes by two-dimensional electrophoresis and matrix-assisted laser desorption/ionization-time of flight analysis

| Spot no. | Accession no. | Protein name | Score | Theoretical kDa/pI | Sequence coverage (%) | MP/TP[a] | Fold ratio[b] |
|---|---|---|---|---|---|---|---|
| Mitochondrial metabolism | | | | | | | |
| 1 | gi\|25144756 | ATP synthase subunit family (ATP-2) | 82 | 57/5.52 | 33 | 15/60 | 2.2 ↓ |
| 2 | gi\|17557712 | ATP synthase subunit family (ATP-5) | 98 | 22/6.67 | 52 | 10/60 | 2.5 ↓ |
| 3 | gi\|17561440 | TS elongation factor (TSFM-1) | 60 | 34/6.27 | 34 | 11/60 | 2.0 ↓ |
| 4 | gi\|17556919 | Pyruvate dehydrogenase kinase family (PDHK-2) | 61 | 45/6.02 | 31 | 12/60 | 2.5 ↓ |
| Glycolytic metabolism | | | | | | | |
| 5 | gi\|71996708 | Glucose-6-phosphate isomerase family (GPI-1) | 165 | 65/6.08 | 35 | 16/60 | 3.4 ↑ |
| 6 | gi\|17535107 | Lactate dehydrogenase family (LDH-1) | 89 | 36/6.42 | 37 | 13/60 | 4.9 ↑ |
| 7 | gi\|32566163 | Glyceraldehyde 3-phosphate dehydrogenase (GPD-2) | 144 | 36/6.76 | 52 | 18/60 | 2.0 ↓ |
| 8 | gi\|1703238 | Fructose-bisphosphate aldolase 1 (Aldolase CE-1) | 114 | 39/6.26 | 40 | 16/60 | 3.6 ↓ |
| Ethanol metabolism | | | | | | | |
| 9 | gi\|17562582 | Sorbitol dehydrogenase family (SODH-1) | 136 | 38/6.07 | 48 | 17/60 | 4.2 ↑ |
| 10 | gi\|25144435 | Aldehyde dehydrogenase family (ALH-1) | 153 | 55/7.14 | 28 | 23/60 | 4.1 ↑ |
| 11 | gi\|17538498 | S-adenosylmethionine synthetase (SAMS-4) | 117 | 44/5.87 | 40 | 14/60 | 4.5 ↑ |
| Oxidative stress resistance | | | | | | | |
| 12 | gi\|71981879 | Superoxide dismutase family (SOD-1) | 68 | 16/6.14 | 57 | 7/60 | 2.2 ↓ |
| 13 | gi\|32565758 | Glutathione S-transferase family (GST-4) | 56 | 25/5.47 | 44 | 7/60 | 2.1 ↓ |
| 14 | gi\|32565831 | Peroxiredoxin family (PRDX-2) | 87 | 21/5.53 | 51 | 11/60 | 2.1 ↓ |
| 15 | gi\|17506189 | Gamma-glutamyltransferase (C53D5.5) | 66 | 70/5.78 | 17 | 12/60 | 4.0 ↓ |
| 16 | gi\|25147792 | Catalase family (CTL-1) | 95 | 57/6.45 | 29 | 14/57 | 2.0 ↓ |
| 17 | gi\|25151141 | Catalase family (CTL-3) | 120 | 59/6.41 | 33 | 16/57 | 3.7 ↓ |
| 18 | gi\|17563248 | ATPase-like family member (rpt-1) | 55 | 48/6.08 | 40 | 13/72 | 4.2 ↑ |
| 19 | gi\|17536181 | Cytochrome P450 family member (cyp-13A8) | 44 | 58/8.38 | 21 | 8/44 | 5.0 ↑ |
| Other | | | | | | | |
| 20 | gi\|17506493 | Elongation factor family (EFT-2) | 57 | 95/6.10 | 18 | 14/60 | 6.2 ↑ |
| 21 | gi\|17508687 | Ribosomal protein, small subunit family member (rps-6) | 58 | 28/10.26 | 30 | 9/60 | 11.5 ↓ |
| 22 | gi\|32563802 | Neuronal symmetry family member (nsy-1) | 67 | 162/6.07 | 15 | 19/56 | 8.0 ↓ |

[a]Number of matched peptides and total searched peptides, [b]n = 3, three independent experiments.

*lbp-5*(*tm1618*) mutant. From this experiment, we were able to identify 199 protein spots by MALDI-TOF MS analysis. Some of those differentially expressed proteins were further verified by qRT-PCR. Table 1 outlines 22 representative genes that were differentially expressed by at least 2-fold in the *lbp-5* mutant strain at both the protein and mRNA levels (in three independent experiments). Fig. 2 shows the qRT-PCR data sorted by different functional groups selected from the proteomics data. Changes in the expression levels of genes involved in glycolytic reactions and mitochondrial energy production are consistent with the novel metabolic adaptation of *lbp-5*-deficient *C. elegans* (Table 1). For example, most mitochondrial proteins (ATP-2, ATP-5, TSFM-1, and PDHK-2) were decreased by 2.0- to 2.5-fold, whereas ALH-1, which acts in ethanol oxidation, was increased by 4.1-fold. In particular, the expression levels of LDH-1 (4.9-fold) and GPI-1 (3.4-fold), which are involved in glycolysis, were increased substantially, whereas those of GPD-2 and aldolase, which are involved in side reactions of glycolysis, were decreased by 2.0- and 3.6-fold, respectively. These results confirm earlier findings that glycolysis is activated (Fig. 1C-E) when the mitochondrial energy cycle (TCA) is attenuated (Fig. 1A and B). These differential expression profile data elucidate the novel metabolic adaptation of *C. elegans*, in which glycolysis is activated to compensate for the energy shortage due to the insufficient mitochondrial β-oxidation/TCA cycle in *lbp-5*(*tm1618*) mutant worms (Table 1, Fig. 2A and B). For instance, the proteomics and qRT-PCR data show that the mutant had decreased expression levels of acyl-CoA dehydrogenase (*acdh*), which catalyzes the first step of fatty acid β-oxidation and thus, plays a key role in energy production. The expression levels of fatty acyl-CoA synthetase (*acs*) and acetyl-CoA acetyl transferase (*B0303.3*) catalyzing the production of acetyl-CoA, a key product of fatty acid β-oxidation, were also decreased. Decreased levels of these enzymes indicate reduced fatty acid β-oxidation in the mitochondria. Down-regulation of *atp-2* and *atp-5*, which encode subunits of complex V of the mitochondrial respiratory chain, also reflects lower TCA activity. Decreased was PDHK-2, which negatively regulates the pyruvate dehydrogenase complex (10, 11). This catalysis blocks the use of the metabolic fuel from the TCA cycle (Table 1) by initiating the conversion of glycolytic products into fatty acids, resulting in the

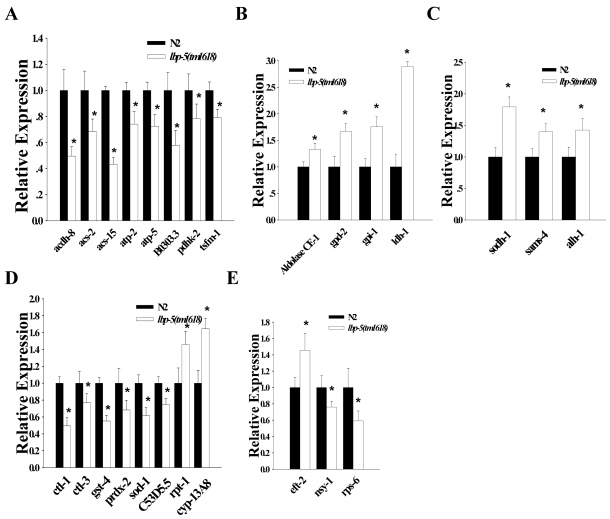


**Fig. 2.** Gene expression in *lbp-5*(*tm1618*) mutant worms. (A) Quantitative reverse transcription–polymerase chain reaction (qRT-PCR) analysis (20) of genes related to mitochondrial energy metabolism in *lbp-5*(*tm1618*) and control N2 worms. The mRNA level of each gene was normalized to actin and presented as the ratio of expression in *lbp-5*(*tm1618*) to control worms. Shown here are: *acdh* (acyl-CoA dehydrogenase)-*8*, *acs-2*, and *acs-15*; *atp* (ATP synthase)-2 and *atp-5*; *B0303.3* (thiolase), *pdhk* (pyruvate dehydrogenase kinase)-2, and *tsmf* (TS elongation factor)-*1*. The data represent the average of triplicate measurements from three samples per experimental group. *P < 0.05 as calculated by Student's t-test versus the control sample. (B) Quantitative RT-PCR of genes related to glycolysis in *lbp-5*(*tm1618*) and control N2 worms. The mRNA level of each gene was normalized to actin and presented as the ratio of expression in *lbp-5*(*tm1618*) to that in control worms. Shown here are: *aldolase CE-1* (fructose-bisphosphate aldolase), *gpd* (glyceraldehyde 3-phosphate dehydrogenase)-*2*, *gpi* (glucose-6-phosphate isomerase)-*1*, and *ldh* (lactate dehydrogenase)-*1*. The data represent the average of triplicate measurements from three samples per experimental group. *P < 0.05 as calculated by Student's *t*-test versus the control sample. (C) Quantitative RT-PCR analysis of genes related to ethanol metabolism in *lbp-5*(*tm1618*) and control N2 worms. The mRNA level of each gene was normalized to actin and presented as the ratio of expression in *lbp-5*(*tm1618*) to that in control worms. Shown here are: *sodh* (sorbitol dehydrogenase)-*1*, *sams* (S-adenosylmethionine synthetase)-*4*, and *alh* (aldehyde dehydrogenase)-*1*. (D) Quantitative RT-PCR analysis of genes involved in oxidative stress in *lbp-5*(*tm1618*) and control N2 worms. Shown here are: *ctl* (catalase)-*1* and *ctl-3*, *gst* (putative glutathione-requiring prostaglandin D synthase)-*4*, *prdx* (peroxiredoxin)-*2*, *sod* (superoxide dismutase)-*1*, *C53D5.5* (γ-glutamyltransferase), *rpt-1* (ATPase-like family member), and *cyp-13A8* (cytochrome P450 family member). The mRNA level of each gene was normalized to actin and presented as the ratio of expression in *lbp-5*(*tm1618*) to that in control worms. (E) Quantitative RT-PCR analysis of other functional genes in *lbp-5*(*tm1618*) and control N2 worms. Shown here are: *eft-2* (elongation factor family), *nsy-1* (neuronal symmetry family member), and *rps-6* (ribosomal protein, small subunit family member). The mRNA level of each gene was normalized to actin and presented as the ratio of expression in *lbp-5*(*tm1618*) to that in control worms. The data represent the average of triplicate measurements from three samples per experimental group.*P < 0.05 as calculated by Student's t-test versus the control sample.

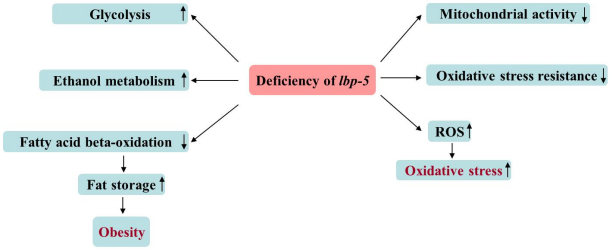


**Fig. 3.** Summary of metabolic consequences of *lbp-5*deficiency. Deletion of *lbp-5* decreases mitochondrial activity but increases glycolysis and ethanol metabolism. In addition, *lbp-5*gene deficiency increases ROS production and decreases oxidative stress resistance. Fat accumulation in *lbp-5*(*tm1618*) mutant nematodes was most likely be due to the down-regulation of fatty acid β-oxidation.

biosynthesis of more fatty acids and triglyceride (fat accumulation) (11). In contrast, the expression levels of several genes related to glycolysis (e.g., *ldh-1*) were increased (Fig. 2B). LDH, which catalyzes the irreversible last step of aerobic glycolysis, can be used as an indicator of glycolytic activity. These results are consistent with our biochemical results (Fig. 1). Together with the observed decrease in ΔΨm, these data explain the basis of the novel metabolic adaptation caused by *lbp-5* deficiency.

Regarding increased ROS production in the *lbp-5*(*tm1618*) mutant, the net effect from the decreased abundance of anti-oxidative enzymes (e.g., GST-4, PRDX-2, CTL-1, and CTL-3) and increased expression levels of oxidation-related enzymes (e.g., SAMS-4, EFT-2, cyp-13A8, and rpt-1) seemingly increased the ROS production and reduced the oxidative stress resistance in *lbp-5*(*tm1618*) mutant worms (Table 1, Fig. 1H and 2D). The amounts of ethanol metabolism-related enzymes (SODH-1 and ALH-1) were greatly increased (4.1- to 4.2-fold), producing more oxidative products due to the reduction in mitochondrial function. Thus, up-regulation of both glycolysis and ethanol metabolism may compensate for the attenuation of mitochondrial function (Fig. 2 and Table 1). Both the qRT-PCR and proteomics profile data are consistent with our hypothesis that *lbp-5* deficiency causes a unique metabolic adaptation in this nematode (Fig. 3).

## DISCUSSION

This study was designed to understand the potential effect of *lbp-5* gene mutation on metabolic pathway by use of biochemical assays and proteomic analysis. Our data suggest that disruption of the *lbp-5* gene not only attenuated mitochondrial function but also enhanced aerobic glycolysis as indicated by lactate accumulation. Core metabolic pathways have been generally well conserved among eukaryotes from yeast to mammals, which use both glycolytic and mitochondrial metabolism depending on extracellular conditions and cues, cel-

lular needs, and the stage of metabolic or circadian cycle (12). For example, fat metabolism in *C. elegans* occurs through a complex network that includes those genes involved in neural signaling, fatty acid uptake, intracellular transport, storage, and consumption (1).

The evolutionarily conserved intracellular lipid-binding proteins FABP and LBP exhibit different functions in energy homeostasis (5, 6, 9). Multiple sequence alignment and phylogenetic analysis of the nematode lbp genes indicate that, although the fatty acid-binding domain is highly conserved, the complete sequences and functions are diverse (7). For instance, mutating *lbp-5* had metabolic consequences in the worms (Table 1), and the presence of other LBP homologues in *C. elegans* did not overcome these effects. Our previous work has shown that silencing *lbp-5* induces fat accumulation (7). Moreover, we demonstrate that fat accumulation due to *lbp-5* deficiency is caused in an *nhr-49* dependent manner via effects on some genes involved in mitochondrial and peroxisomal beta-oxidation, fatty acid desaturation/elongation, and gluconeogenesis. In addition, similar to PPAR-α-deficient mice, *nhr-49* mutant worms exhibit a decrease in glucose and increase in lactate concentrations (13). These data suggest that LBP-5 and NHR-49 may work together as functional partners in lipid metabolism. However, this relationship should be investigated further before we conclude that the metabolic adaptation is mainly caused by reduced NHR-49 function.

The changes in expression levels of genes associated with various metabolic pathways (e.g., mitochondrial energy production, glycolysis, fat accumulation, ROS generation, ethanol metabolism, and oxidative stress resistance) in *lbp-5*(*tm1618*) (Fig. 3) indicate a classical metabolic adaptation in which glycolysis is promoted. Generally, pyruvate has one of three metabolic fates: to become acetyl-CoA for consumption in the TCA cycle, to become ethanol, or to become lactate. Thus, up-regulation of both glycolysis and ethanol metabolism may compensate for the attenuation of mitochondrial function.

Although there were some differences in the magnitude of the changes in the expression levels of certain proteins involved in glycolysis (e.g., GPD-2 and aldolase) between the proteomic analysis and qRT-PCR data, the overall transcription profile data indicate how cellular metabolism is redirected from the mitochondrial β-oxidation/TCA cycle to glycolysis in *lbp-5*(*tm1618*) mutant worms (Fig. 2). In fact, differences between mRNA and protein levels of a particular gene are not uncommon (14). The genes listed in Table 1 were analyzed at both the mRNA and protein levels to ensure that the pattern of changes in a certain group of genes and their corresponding proteins were consistent in response to *lbp-5* gene mutation.

A major readout of cell status is the level of ROS. Down-regulations of *atp-2* and *atp-5* also indicate attenuated mitochondrial function, which can decrease the production of ROS in the *lbp-5*(*tm1618*) mutant (Fig. 2A). However, ROS levels in the *lbp-5* mutant were paradoxically higher than those of the control, supporting the likelihood that some sort of mitochondrial uncoupling had occurred in the *lbp-5* mutant. Yet, higher levels of ROS may be more likely caused by the decrease in anti-oxidative genes rather than increased mitochondrial activity, resulting in reduced oxidative stress resistance in *lbp-5*(*tm1618*) mutant worms (Table 1 and Fig. 2D). For instance, the expression levels of catalases (*ctl-1*, *ctl-3*) and *sod-1* were decreased in the *lbp-5* mutant, which were also seen in the 2D data (Table 1). However, the exact cause of these changes requires further investigation.

The most notable effect of *lbp-5* deficiency is fat accumulation (7), which can be due to storage signals or reduced lipolysis. When cells encounter insufficient amounts of mobilized fatty acids due to *lbp-5* deficiency, a certain energy-sensing system yet to be identified responds to the diminished mitochondrial metabolism and initiates the compensatory activation of glycolysis. This activation may divert glycolytic products into biosynthetic pathways, such as the pentose phosphate pathway, leading to fatty acid biosynthesis.

LBP-5 protein is expressed widely in many different cell types. In particular, LBP-5 expression is high in the hypodermis and intestine, which are major sites of fat accumulation. LBP-GFP fusion protein expression was observed during embryogenesis and in all subsequent larval and adult stages (7), suggesting that LBP-5 most likely plays important roles throughout development. Thus, the broad cellular distribution of LBP-5 expression may provide valuable information about how LBP-5 reduces glycolysis in the life cycle of a normal worm.

In conclusion, our data reveal that LBP-5 plays a regulatory role in *the* energy homeostasis of *C. elegans*. The direct consequences of *lbp-5* deficiency are fat accumulation and ROS production and reduced $\Delta\Psi m$ and anti-oxidation activity. More importantly, *lbp-5* mutation leads to a classical metabolic adaptation in which glycolysis is activated and the mitochondrial TCA cycle is suppressed, but this finding needs to be confirmed through additional experiments. Thus, cellular lipid transport proteins, particularly LBP-5, are important subjects of research on obesity and metabolic diseases (15).

## MATERIALS AND METHODS

### Deoxyglucose (DOG) treatment

Details on the maintenance of strains, mitochondrial assays, and LDH activity analysis are described in Supplemental Information. For DOG treatment, synchronized L1 stage worms were grown to L4 stage, as described previously in (16). Next, nematodes were transferred to plates containing 25 μM 5-fluoro-2′-deoxyuridine (Sigma-Aldrich) to prevent progeny formation. After incubation for 16 h at 20°C, the worms were transferred to plates containing 5 mM DOG and cultured for another 48 h at 20°C. NGM agar plates without DOG were used as control. Worms were harvested by washing three times with a ice-cold M9 buffer to separate the nematodes from bacteria. Nematodes were frozen in liquid nitrogen and stored at −80°C until further processing. Worm extracts were

prepared as described (17,21).

### Paraquat resistance

Synchronized L1-stage worms were grown on normal NGM plates until their progeny reached L4 stage, as previously described (22). A total of 50 worms were transferred to NGM plates with 4 mM paraquat and incubated for 72 h at 20°C, after which the number of surviving worms was counted. The data represent the mean ± standard deviation from triplicate measurements obtained from three independent experiments.

### Statistical analyses

Statistical significance was determined using Student's *t*-test (SPSS 16.0, SPSS, Inc., Chicago, IL). Results with P values less than 0.05 were deemed statistically significant.

### Acknowledgements

We thank the Caenorhabditis Genetics Center for providing strains. This work was supported by grants from the National Research Foundation of Korea (2011-0028112), and the National Project for Personalized Genomic Medicine (A111218-11 to Y.-K.P.).

## REFERENCES

1. Watts, J. L. (2009) Fat synthesis and adiposity regulation in Caenorhabditis elegans. *Trends. Endocrinol. Metab.* **20**, 58-65.
2. Kniazeva, M., Euler, T. and Han, M. (2008) A branched-chain fatty acid is involved in post-embryonic growth control in parallel to the insulin receptor pathway and its biosynthesis is feedback-regulated in C. elegans. *Genes Dev.* **22**, 2102-2110.
3. Owada, Y. (2008) Fatty acid binding protein: Localization and functional significance in the brain. *Tohoku J. Exp. Med.* **214**, 213-220.
4. Esteves, A. and Ehrlich, R. (2006) Invertebrate intracellular fatty acid binding proteins. *Comp. Biochem. Physiol. C. Toxicol. Pharmacol.* **142**, 262-274.
5. Haunerland, N. H. and Spener, F. (2004) Fatty acid-binding proteins- -insights from genetic manipulations. *Prog. Lipid. Res.* **43**, 328-349.
6. Storch, J. and McDermott, L. (2009) Structural and functional analysis of fatty acid-binding proteins. *J. Lipid. Res.* **50 (Suppl)**, S126-131.
7. Xu, M., Joo, H. J. and Paik, Y. K. (2011) Novel functions of lipid-binding protein 5 in Caenorhabditis elegans fat metabolism. *J. Biol. Chem.* **286**, 28111-28118.
8. Zuryn, S., Kuang, J. and Ebert, P. (2008) Mitochondrial modulation of phosphine toxicity and resistance in Caenorhabditis elegans. *Toxicol. Sci.* **102**, 179-186.
9. Schroeder, F., Jolly, C. A., Cho, T. H. and Frolov, A. (1998) Fatty acid binding protein isoforms: structure and function. *Chem. Phys. Lipids.* **92**, 1-25.
10. Holness, M. J. and Sugden, M. C. (2003) Regulation of pyruvate dehydrogenase complex activity by reversible phosphorylation. *Biochem. Soc. Trans.* **31**, 1143-1151.
11. Kim, S., Shin, E. J., Hahm, J. H., Park, P. J., Hwang, J. E. and Paik, Y. K. (2012) PDHK-2 deficiency is associated with attenuation of lipase-mediated fat consumption for the increased survival of Caenorhabditis elegans dauers. *PLoS One* **7**, e41755.
12. Sahar, S. and Sassone-Corsi, P. (2009) Metabolism and cancer: the circadian clock connection. *Nat. Rev. Cancer* **9**, 886-896.
13. Atherton, H. J., Jones, O. A., Malik, S., Miska, E. A. and Griffin, J. L. (2008) A comparative metabolomic study of NHR-49 in Caenorhabditis elegans and PPAR-alpha in the mouse. *FEBS Lett.* **582**, 1661-1666.
14. Gygi, S. P., Rochon, Y., Franza, B. R. and Aebersold, R. (1999) Correlation between protein and mRNA abundance in yeast. *Mol. Cell Biol.* **19**, 1720-1730.
15. Baretic, M. (2012) Targets for medical therapy in obesity. *Dig. Dis.* **30**, 168-172.
16. Curran, S. P. and Ruvkun, G. (2007) Lifespan regulation by evolutionarily conserved genes essential for viability. *PLoS Genet* **3**, e56.
17. Choi, B. K., Chitwood, D. J. and Paik, Y. K. (2003) Proteomic changes during disturbance of cholesterol metabolism by azacoprostane treatment in Caenorhabditis elegans. *Mol. Cell Proteomics.* **2**, 1086-1095.
18. Park, S. O., Kim, H. L., Lee, S. W. and Park, Y. S. (2013) Tetrahydropteridines possess antioxidant roles to guard against glucose-induced oxid ative stress in Dictyostelium discoideum. *BMB Rep.* **46**, 86-91.
19. Cho, J. H., Lee, P. Y., Son, W. C., Chi, S. W., Park, B. C., Kim, J. H. and Park, S. G. (2013) Identification of the novel substrates for caspase-6 in apoptosis using proteomic approaches. *BMB Rep.* **46**, 588-593.
20. Lee, E., Jeong, K. W., Shin, A., Jin, B., Jnawali, H. N., Jun, B. H., Lee, J. Y., Heo, Y. S. and Kim, Y. (2013) Binding model for eriodictyol to Jun-N terminal kinase and its anti-inflammatory signaling pathway. *BMB Rep.* **46**, 594-599.
21. Li, Y. and Paik, Y. K. (2011) A potential role for fatty acid biosynthesis genes during molting and cuticle formation in Caenorhabditis elegans. *BMB Rep.* **44**, 285-290.
22. Yang, W., Li, J. and Hekimi, S. (2007) A Measurable increase in oxidative damage due to reduction in superoxide detoxification fails to shorten the life span of long-lived mitochondrial mutants of Caenorhabditis elegans. *Genetics* **177**, 2063-2074.